

1 Transformations in Exposure to Debris Flows in Post-Earthquake Sichuan, 2 China

3
4 Isabelle Utley¹, Tristram Hales¹, Ekbal Hussain², Xuanmei Fan³

5
6 [1] School of Earth and Environmental Sciences, Cardiff University, Cardiff, CF10 3AT, UK.

7 [2] British Geological Survey, Keyworth, Nottingham, NG12 5GG, UK

8 [3] State Key laboratory of Geohazard Prevention, Chengdu University of Technology, Chengdu, China

9
10 *Correspondence to: Isabelle E.K Utley (utleyieu@gmail.com)*

11
12 **Abstract.** Post-earthquake debris flows can exceed volumes of $1 \times 10^6 \text{m}^3$ and pose significant challenges to
13 downslope recovery zones. These stochastic hazards form when intense rain remobilises coseismic landslide
14 material. As communities recover from earthquakes they mitigate the effects of these debris flows through
15 modifications to catchments such as building check dams and levees. We investigate how different catchment
16 interventions change exposure and hazard of post-2008 debris flows in three gullies in Sichuan province, China.
17 These were selected based on the number of post-earthquake check dams – Cutou (2), Chediguan (2) and Xiaojia
18 (none). Using high resolution satellite images, we developed a multitemporal building inventory from 2005 to
19 2019, comparing it to spatial distribution of previous debris flows and future modelled events. Post-earthquake
20 urban development in Cutou and Chediguan increased exposure to a major debris flow in 2019 with inundation
21 impacting 40% and 7% of surveyed structures respectively. We simulated future debris flow runouts using
22 LAHARZ to investigate the role of check dams in mitigating three flow volumes – 10^4m^3 (low), 10^5m^3 (high)
23 and 10^6m^3 (extreme). Our simulations show check dams effectively mitigate exposure to low and high flow
24 events but prove ineffective for extreme events with 59% of buildings in Cutou, 22% in Chediguan and 33% in
25 Xiaojia significantly affected. We verified our analyses through employing a statistical exposure model, adapted
26 from a social vulnerability equation. Cutou's exposure increased by 64% in 2019, Chediguan's by 52% whilst
27 only 2% for Xiaojia in 2011, highlighting that extensive grey infrastructure correlates with higher exposure to
28 extreme debris flows, but less so to smaller events. Our work suggests that the presence of check dams contributes
29 to a perceived reduction in downstream exposure. However, this perception can lead to a levee effect, whereby
30 exposure to larger, less frequent events is ultimately increased.

31 **Keywords**

32 Debris Flows, Built Environment, Exposure, Check dams, LAHARZ.

33 **1. Introduction**

34
35
36 Major earthquakes such as the 1994 M_w 6.8 event in Northridge, California (Harp and Jibson, 1996) and the 1999
37 M_w 7.3 earthquake in Chi-Chi, Taiwan (Liu et al., 2008) have triggered chains of hazards that increase the exposure
38 of local communities to secondary hazards for many years after the initial disaster. Following the 2008 M_w 7.9
39 Wenchuan earthquake in Sichuan, China, debris flows occurred more frequently and at a higher magnitude ($>1 \times$
40 10^6m^3) after the earthquake compared to flows before the earthquake (Cruden and Varnes., 1996; Cui et al., 2008;
41 Huang and Li., 2009; Guo et al., 2016; Thouret et al., 2020). Increased debris flow frequency impacts vulnerable
42 communities and local infrastructure, potentially reshaping the demographic and structural landscape of
43 previously rural regions (Chen et al., 2011). The frequency of post-seismic flows is heavily influenced by sediment
44 availability, often controlled by coseismic landslide distribution, hydrology, and slope (Horton et al., 2019). The
45 ready transformation and remobilisation of seismically loosened deposits into water-laden sediments leads to a
46 heightened probability of debris flow hazards for extended periods, further exacerbating the potential impacts felt
47 by these areas (Costa et al., 1984; Huang & Li, 2014; Fan et al., 2019b).

48
49
50 Post-seismic debris flows affect the expanding built environment and communities located in the flat land that
51 forms along floodplains and on debris and alluvial fans. In addition to direct loss of life, debris flows repeatedly
52 block and/or destroy rivers, roads, tunnels, and bridges, and damage property and agriculture, and result in loss of
53 life (Chen, N et al., 2011). Buildings are particularly susceptible to the impacts of debris flows (Hu et al., 2012;
54 Zeng et al., 2015), with property damage accounting for nearly all impacts such as casualties and fatalities (Wei
55 et al., 2018; Wei et al., 2022). Variations in construction materials are a particularly important factor in
56 determining structural resilience and vulnerability to debris flows (Zhang, S et al., 2018). Despite focus on
57 building resilience and reducing vulnerability, post-earthquake regions are often areas of significant rebuilding

58 and expansion of infrastructure so the exposure to debris flows changes rapidly in these areas. The development
59 of critical infrastructure such as highways and tunnels further encourages the growth of the built environment and
60 subsequent influx of people settling in areas exposed to geological hazards (Cruden and Varnes, 1996; Jiang et
61 al., 2016).

62
63 Check dams are a common form of risk mitigation for debris flows globally (Zeng et al., 2009; Peng et al., 2014;
64 Cucchiaro, S. et al., 2019b), and one that is prevalent in post-earthquake Wenchuan (Chen, X. et al., 2015; Guo
65 et al., 2016). Check dams store debris flow sediment, locally reduce channel slope, and are often permeable to
66 affect debris flow hydrology. However, they have disadvantages such as requiring regular maintenance (to reduce
67 sediment inputs) (Kean et al., 2018). The mitigation potential of these structures is contingent on their position
68 along a channel, their height, amount of sediment fill, and their strength (which depends on the materials used for
69 construction) (Dai et al., 2017). These factors evolve through time, meaning that the hazard-mitigating factor of
70 check dams can vary with time and often with unpredictable results. The presence of check dams changes the
71 downstream risk, primarily by altering the magnitude and frequency distribution of debris flows within the
72 channel. For well-made check dams of sufficient volume to mitigate the largest debris flows, this can reduce the
73 downstream risk of debris flows to negligible by effectively mitigating the entire hazard. However, in the case of
74 the Wenchuan region, check dams are rarely large enough or regularly cleared of sediment to mitigate the largest
75 debris flows, which can exceed 10^6 m^3 in volume.

76
77 The presence of check dams, particularly in drainage basins with a limited history of catastrophic debris flow
78 events, may affect the perception of risk downstream. They serve to stabilize, obstruct, drain, and/or halt the
79 movement of flows (Hübl and Fiebigger., 2005; Chen et al., 2015). The perception that check dams have mitigated
80 all hazards may promote the expansion of infrastructure into floodplains and debris fans, potentially increasing
81 exposure to debris flows that overtop dams or occur due to dam failure. The increase of exposure is common on
82 floodplains where the presence of flood control levees can promote building onto floodplains – a process known
83 as the levee effect (Collenteur et al., 2015). In the flooding example, the presence of levees reduces the frequency
84 of small and medium sized floods, but when large floods occur that cause those levees to fail, heightened
85 floodplain exposure can lead to higher damage. The effect of check dams on risk perception is less well
86 understood. Anecdotal examples from the Wenchuan region (e.g., Hongchun, Taoguan gullies) show that large
87 debris flow events in 2010, 2013 and 2019 caused significant damage despite the presence of check dams (Dai et
88 al., 2017). However, it is not clear if the presence of check dams affected exposure relative to the large-scale
89 expansion of infrastructure in the post-earthquake recovery phase.

90
91 This study seeks to understand whether the addition of engineered mitigation measures, primarily check dams,
92 have influenced the susceptibility of post-earthquake Wenchuan communities to large debris flows. We compare
93 3 catchments with similar topography and geology, but different levels of mitigation. We measure the building
94 exposure in two neighbouring catchments with check dams (Cutou and Chediguan) and compare with a third,
95 unmitigated gully (Xiaojia). We examine how infrastructure develops in the basins with time and as a function of
96 check dam measures. By analysing infrastructure development in these catchments, particularly in Cutou and
97 Chediguan in the years following mitigation – will seek to assess how check dam construction has impacted
98 infrastructure growth and the potential exposure to debris flow events of different sizes. Additionally, our analysis
99 will explore whether the presence of these structures has impacted risk perception and/or land-use decisions in
100 ‘at-risk’ catchments.

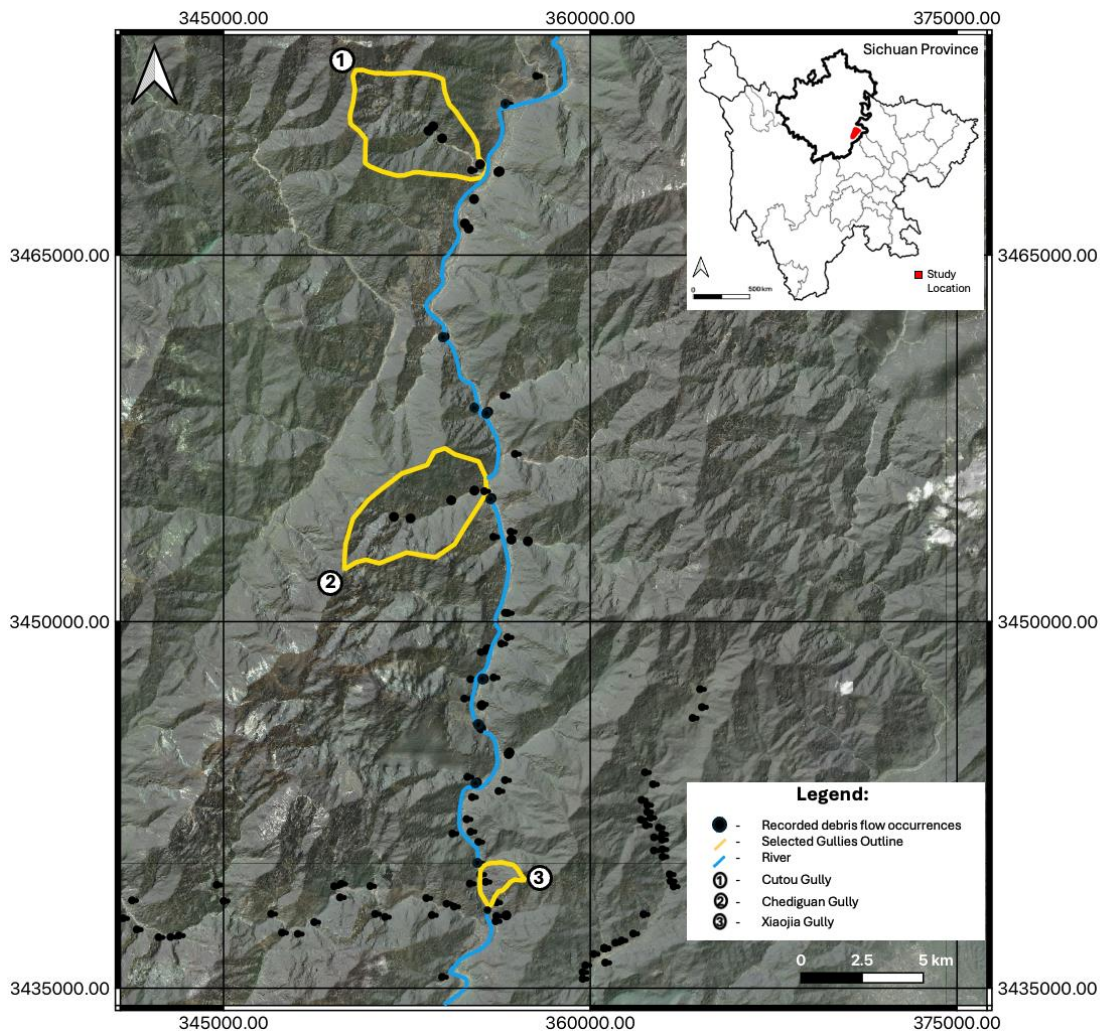
101 102 103 **2. Study Area: Sichuan Province, China**

104 China’s mountainous regions, including the Longmenshan, account for 69% of the country’s land mass with over
105 a third of the population living in these regions (Chen et al., 2011; He et al., 2022). 72% of this landscape suffers
106 from debris flow activity. Between 2005 and 2018, estimates suggest over 800 debris flow occurrences each year
107 (He et al., 2022; Wei et al., 2021) Following the 2008 Wenchuan Earthquake, landslides were widely recorded
108 across both northern and southern provinces, with debris flows particularly concentrated in the steep terrain of
109 southern Sichuan. However, debris flows, and other landslide types have since been documented across a broad
110 range of regions in China (Liu et al., 2018). The 2008 Mw 7.9 Wenchuan earthquake primarily impacted Sichuan
111 province (Fig 1). The epicentre was located near Yinxiu, Wenchuan County, within the seismically active
112 Longmenshan Fault Zone (Li et al., 2019). The shaking triggered around 56,000 landslides and displaced nearly
113 3 km^3 of loose material (Fan et al., 2018; Luo et al, 2020). In subsequent years, the unstable material has been
114 reactivated as debris flows, many of which exceed 10^6 m^3 in mobilised volume (Frances et al., 2022). The risk
115 from these debris flows has been compounded by increasing exposure due to China’s rapid rural development
116 programme, which includes the construction of roads, bridges, and industrial facilities (Tang et al., 2022).

118 Four significant episodes of debris flows occurred in the post-earthquake Wenchuan region in 2008, 2010, 2013
 119 and 2019 (Tang et al., 2022; Fan et al., 2019b). Each event was associated with monsoon rainfall that occurred in
 120 different parts of the range. The largest flow surges, containing millions of cubic meters of sediment were located
 121 in the gullies along the Minjiang in Sichuan. Large scale flooding further amplified the impacts, for example in
 122 Yingxiu Town, Wenchuan County (Liu et al., 2016b). Debris flow events occurring post-earthquake often exhibit
 123 larger material volumes compared to flow events recorded prior to 2008. Horton et al., (2019) attributed the
 124 increase in flow volume too high in channel sediment volumes that can drive bulking. The resulting increase in
 125 debris flow hazards necessitated engineered mitigation measures to reduce risk levels in the basin communities
 126 (Tang et al., 2009; Huang et al., 2009; Huang, 2012).

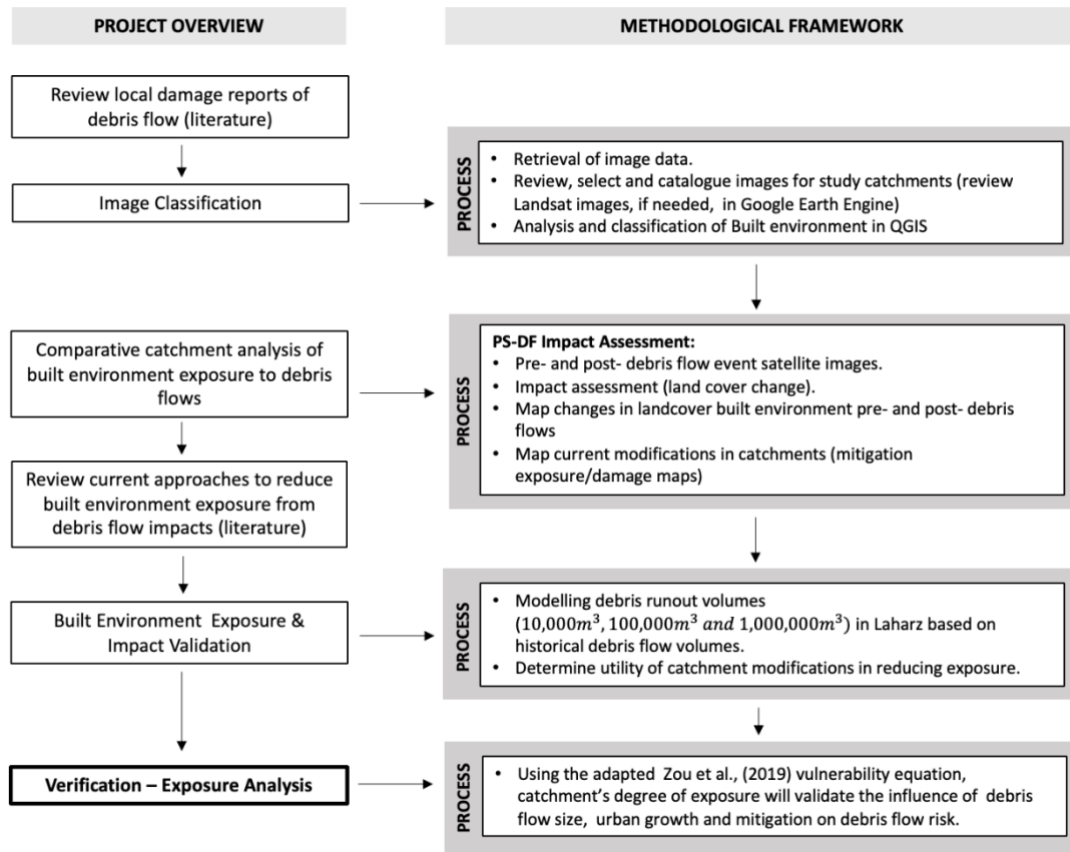
128 In this study we focus on three gullies along the Minjiang - Cutou, Chediguan and Xiaojia and debris flow events
 129 on August 20th, 2019, and 4th July 2011 (Fig 1). Cumulative rainfall on 20th August 2019 peaked at 83 mm in
 130 Cutou and 65 mm in Chediguan resulting in large debris flows measuring over $50 \times 10^4 \text{ m}^3$ in each gully. Cutou
 131 gully is known for its high frequency of post-seismic debris flows, which has been attributed to the total of 11×10^6
 132 m^3 coseismic deposits generated by the earthquake (Yan et al 2014). Although a check dam was built in 2011 to
 133 manage debris flow impacts in Chediguan gully a large damaging debris flow of $64 \times 10^4 \text{ m}^3$ occurred on 20 August
 134 2019 and destroyed the drainage groove and G213 Taiping Middle Bridge (Li et al., 2021). The debris briefly
 135 blocked river flow in the Minjiang causing water levels to rise during flood peak. This led to flooding at the
 136 Taipingyi hydropower station located 200 m upstream.

138 Xiaojia gully, is a moderate debris flow hazard area based on limited past occurrences and has no existing
 139 engineered mitigation measures. Following a period of debris flow activity in 2010, and after a period of
 140 continuous heavy rainfall approximately $30,000 \text{ m}^3$ of deposits were remobilised and transported along the channel
 141 to the gully mouth. This event led to a period of disruption on the S303 road from flooding (Liu et al., 2014).



143 **Figure 1:** Location of the three gullies that form the focus of this study within Sichuan Province. Recorded post-
 144 2008 landslide occurrences are from the Wang et al. (2022) multitemporal datasets (© Google Earth 2019).

145
 146 **3. Methodology**



147
 148 **Figure 2:** Schematic of our method. The key data sources comprise three multi-temporal datasets, including two
 149 from Fan et al. (2019a) covering debris flow and triggering rainfalls, as well as mitigation measures. The third
 150 dataset is adapted from Fan et al., (2019a) and highlights gully's with debris flow events post-2008 including
 151 information on the flow volume and presence of mitigation. Additional spatial data sources include aerial imagery
 152 from OpenStreetMap (OpenStreetMap contributors., 2023), World Settlement Footprint (World Settlement
 153 Footprint., 2019) and Shuttle Radar Topography Mission (SRTM) (Farr et al, 2007).

154
 155
 156 **3.1 Data Classification**

157
 158 This study builds on existing multi-temporal debris flow datasets produced by Fan et al., (2019a). Dataset 1 has
 159 an aerial extent of 892 km² and presents the location and dimensions of debris flow events between 2008 and
 160 2020. Dataset 2 presents a list of mitigative actions e.g., construction of check dams, taken between 2008–2011.
 161 We used an SRTM DEM to construct elevation profiles of Cutou, Chediguan and Xiaojia gullies to extract
 162 topographic characteristics to understand the mechanism of slope failure in the event of a rainfall-induced debris
 163 flow. These profiles facilitate morphological valley changes from debris flows to be identified. Through a
 164 comparative analysis of the 20th August 2019 debris flows in Cutou and Chediguan, we investigated the relative
 165 difference in land use change in the two gullies from 2008 to 2019, with a focus on changes before and after the
 166 2019 flow event.

167
 168 Landscape modification from 2005 to 2019 were mapped using high resolution (0.5 to 2.5m) satellite images
 169 (Table 1). We selected images with less than 50% cloud cover and cross-referenced the mapped features with
 170 existing data sources in OpenStreetMap (OpenStreetMap contributors., 2023) and Dynamic World (Brown et al.,
 171 2022). Where satellite imagery was unavailable, we used aerial photos obtained from Google Earth,
 172 OpenStreetMap and World Settlement Footprint (World Settlement Footprint., 2019). It should be acknowledged
 that platforms like OpenStreetMap offer a regional view of Wenchuan rather than a detailed local-scale with

mapping limited to main roads and 150 settlement polygons. However, this study’s locations are unaffected by this due to their position next to the G213 national highway and G4217 road.

Table 1 Satellite and aerial imagery used for data analysis and interpretation of the built environment.

Data ID	Data Source	Acquisition Date	Resolution (m)
Aerial Satellite	Worldview (in QGIS – ‘Satellite’ XYZ tile)	2022	1.0
Satellite	Worldview (in Google Earth Pro., 2023)	10.12.2010 26.04.2011 03.04.2018 29.10.2019	1.0
Satellite	Planet	14.08.2019 24.08.2019	3.0
Satellite	Maxar Technologies (in Google Earth Pro., 2023)	09.09.2005 26.04.2011	3.0
Satellite	CNES/Airbus (in Google Earth Pro., 2023)	15.04.2015	1.0

We used imagery collated from the sources listed in Table 1 to map manufactured features—including buildings, factories, roads, and dams—in order to understand the evolution of the built environment and subsequent human activities since 2005 across Cutou, Chediguan, and Xiaojia. We mapped features corresponding to human activities such as roads and properties. We highlighted at-risk zones in Cutou, Chediguan, and Xiaojia. We focus on spotlighting areas of high debris flow exposure in Cutou and Chediguan, comparing them with Xiaojia to evaluate the efficacy of check dams in mitigating potential debris flow hazards downstream of the dams.

3.2 Modelling Future Debris Flow Runout and Building Exposure

Both Cutou and Chediguan had check dams installed after the 2008 earthquake, while the Xiaojia gully remained unmodified. We compared the impacts of 2019 debris flows in Cutou and Chediguan gullies with a 2011 debris flow event in Xiaojia to identify the effectiveness of artificial dams in mitigating exposure to post-seismic debris flows. By using scenario modelling we identified at which point does the size of the hazard outweigh the mitigative capacity of the check dam to prevent overtopping. We mapped debris flows of differing scales within each of our three catchments using LAHARZ. LAHARZ is a GIS toolkit for lahar hazard mapping and modelling, developed by the USGS to calculate the area of inundation and cross sections based on empirical scaling relationships between area and volume (Schilling., 2014; Iverson et al., 1998). These empirical relationships allow for the creation of realistic inundation areas without a priory knowledge of the rheological parameters. The model simulates a debris flow triggered at a source point located on a digital elevation model and with an initial source volume. The model calculates the flow path downslope of the triggering location then generates a cross-section at each point downslope that represents the depositional volume for that area (Iverson et al., 1998).

We implemented this model using the extension in ArcGIS (Schilling., 2014). We used the 30m resolution DEM as an input, as it is the most reliable of the globally available DEMs. We identified the source areas of 2019 debris flows for Chediguan and Cutou and the 2011 for Xiaojia (Cutou – 351603, 3473449; Chediguan – 350846, 3453894; Xiaojia – 356666, 3439268) from satellite imagery and used these as the triggering locations for our simulations. We then prescribed three input volumes at each of these locations ($10^4 m^3$, $10^5 m^3$ and $10^6 m^3$). The flow volumes simulate a range of observed post-2008 debris flows, representing low, high, and extreme debris flows documented in the Fan et al., (2019a) datasets. The volumes we selected reflects the range of similar hazard events in comparable geomorphological settings such as other parts of China and Italy (Wu et al., 2016; Bernard et al., 2019). For catchments with check dams, we added barriers at each check dam location by raising the cell count of the DEM by the height of the check dam obtained from field imagery.

The model was validated by comparing simulated runout extents with observed debris flows from post-2008 events. While a 30m resolution was the only available DEM for our study locations, we tested the sensitivity of DEM resolution on the extent of the final flow. A higher, 10m resolution DEM was available for the Cutou gully and we ran LAHARZ for that catchment. While the 10m DEM created a more effective flow path compared to the mapped data, the flow depositional area was similar in both the 10m and 30m scenario (RMSE 18m). Given the lack of a significant difference between the two DEM resolution we ran 30m scenarios across the three catchments. We note that there is not a strong understanding currently of what controls the maximum size of debris flows within Wenchuan catchments, hence we cannot attribute a particular probability to each scenario.

In the analysis of post-seismic debris flow, exposure and vulnerability assessments plays a crucial role (Lo et al., 2012). However, adapting traditional vulnerability methods which analyse inherent fragility and the potential loss of elements at risk, both attainable through remote practises, calculating exposure with minimal onsite data, remains a challenge. We adapted a vulnerability model by Zou et al. (2019) to quantify the extent of exposure to the built environment at our three sites, Cutou, Chediguan and Xiaojia.

Utilising satellite and/or aerial imagery and extracting spatial characteristics to identify both elements at risk as well as hazard-affected zones, our analysis facilitates the assessment of regional exposure without relying heavily on data collected onsite. All analysis steps were conducted within a GIS environment. Our model quantifies the susceptibility of the built environment to debris flow damage. The degree of exposure, E_{df} , is expressed as:

$$E_{df} = E_b \times C \pm M \quad (1)$$

E_b is the number of buildings damaged, and C is the fragility index of the elements at risk (Zou et al., 2019). Fragility values range from 0 to +1, with higher values indicating greater susceptibility to damage and/or failure. The assessment was conducted at the individual building level within GIS: building footprints were manually digitised and assigned fragility values based on proximity to debris flow channels and observed damage in previous events alongside literature. Due to limitations in detailed structural data and the reliance on remotely sensed satellite images, we simplified fragility to a binary classification: buildings clearly inundated, damaged or situated in highly susceptible locations (i.e., along the channel or gully mouth) were given a value of 1, all other buildings were set a value of 0. This approach provided us with a robust and replicable framework, avoiding overinterpretation of uncertain data. These values were then validated using historical damage reports, where available, from the 2008 earthquake recovery period to ensure applicability (Zeng et al., 2015; Wei et al., 2021; Petley et al., 2023). This GIS-based approach enables a replicable framework for similar hazard-prone contexts.

The key difference between our method and that of Zou et al (2019) is the incorporation a modification factor, M , to account for the effectiveness of engineered measures like check dams in mitigating building damage and subsequent exposure. The mitigation factor, M , quantifies the influence of engineered measures, in this study check dams, on the vulnerability and subsequent exposure of buildings to debris flow impacts. The addition of this factor brings an evaluative element to the exposure assessment, quantifying the influence of check dams and assigning values ranging from -1.0 to +2.0 to reflect a spectrum of mitigation outcomes:

- $M = -1$: Effective mitigation of debris flows, resulting in a significant reduction in hazard exposure, as evidenced by a decrease in the number of buildings damaged during historical events following construction.
- $M = 0$: No mitigation present; exposure levels are entirely dependent on natural site conditions.
- $M = +1$: Ineffective mitigation; there is no reduction in the number of buildings impacted in recorded debris flow events following dam construction.
- $M = +2$: Mitigation increases exposure. Recorded events of similar volume show an increase in the number of buildings impacted following dam construction.

The above -1 to +2 scale was selected to capture a nuanced relationship between mitigation effectiveness and vulnerability. A reduction in M (e.g., -1) lowers hazard exposure by reducing flow impacts at critical locations, thereby decreasing E_{df} . Conversely, an increase in M (e.g., +2) elevates exposure, as development in hazard-prone areas amplifies the potential for damage. For example, a decrease in M by one unit (from 0 to -1) reflects an improvement in flow attenuation due to effective check dams, reducing overall exposure. Conversely, an increase in M by one unit (from 0 to +1) signifies a scenario where mitigation fails, e.g. the 2019 debris flow event in Cutou, maintaining high exposure levels. At $M = +2$, exposure exceeds natural vulnerability due to increased hazard presence caused by intensified land use near mitigation structures.

This scale was developed through a combination of evaluating present hazard mitigation and analysing of historical data, particularly from the 2008 earthquake recovery. Moreover, this approach, based upon the methodology proposed by Zou et al. (2019), allows for an assessment of exposure by considering both the physical resistance of buildings and the efficacy of mitigation efforts.

4. Results

4.1 Assumptions

280
281
282
283
284
285
286
287
288
289
290

In constructing the building inventory for Cutou and Chediguan, a comprehensive approach was taken to ensure accuracy and completeness. We used aerial and satellite imagery spanning 14 years, with a focus on mapping changes from 2011 to 2019. This involved careful analysis to delineate individual buildings, considering variations in size, shape, and spatial arrangement. Mapping efforts for Xiaojia were limited to 2010-2011 due to suboptimal image quality. Our approach incorporated assumptions regarding structural categorisation, including residential, industrial, and commercial buildings. These assumptions were informed by existing literature on local building typologies and architectural styles (Hao et al., 2013; Hao et al., 2012) and aerial photograph analysis from platforms such as Google Earth and Dynamic World. By amalgamating diverse information sources, we aimed to create a comprehensive inventory that correctly reflects the built environment of the study area.

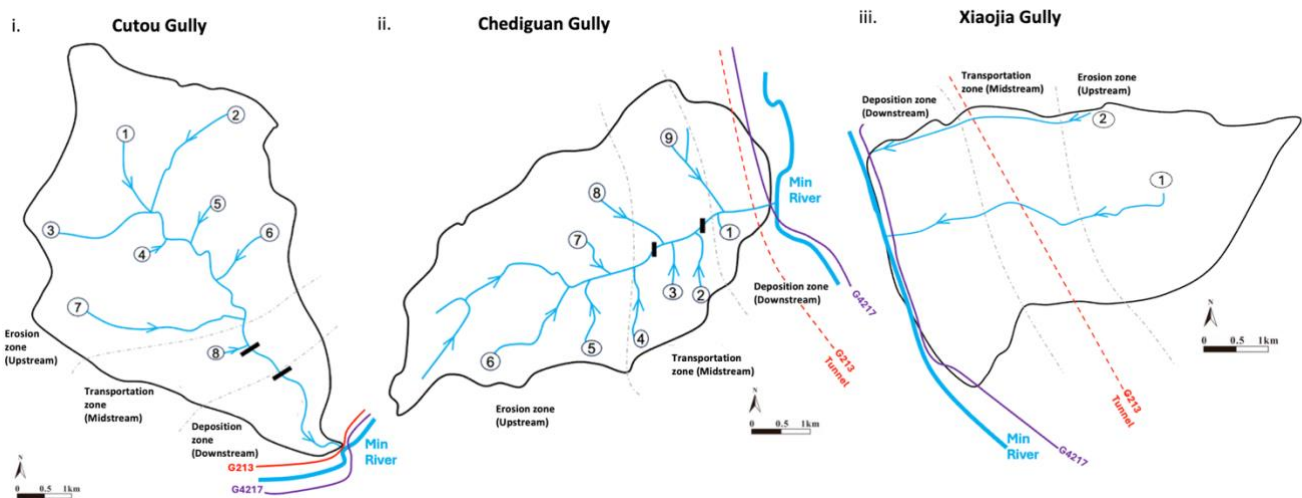
291
292
293
294
295
296
297
298
299

Additionally, we used a 30-meter Digital Elevation Model (DEM) obtained from the SRTM dataset (Farr et al., 2007). However, it is necessary to acknowledge the limitations of this data, particularly its low resolution and subsequent blockiness, which potentially hindered detailed topographical analysis. Despite this, the DEM provided valuable contextual information for understanding the terrain and its influence on building distribution and spatial patterns within the three sites. Furthermore, while using the empirical LAHARZ model for debris flow inundation mapping, we had to account for a degree of approximation in both aerial coverage and debris flow inundation due to the 30m resolution of the DEM file.

300 4.2 Mapping Post-Earthquake Risk

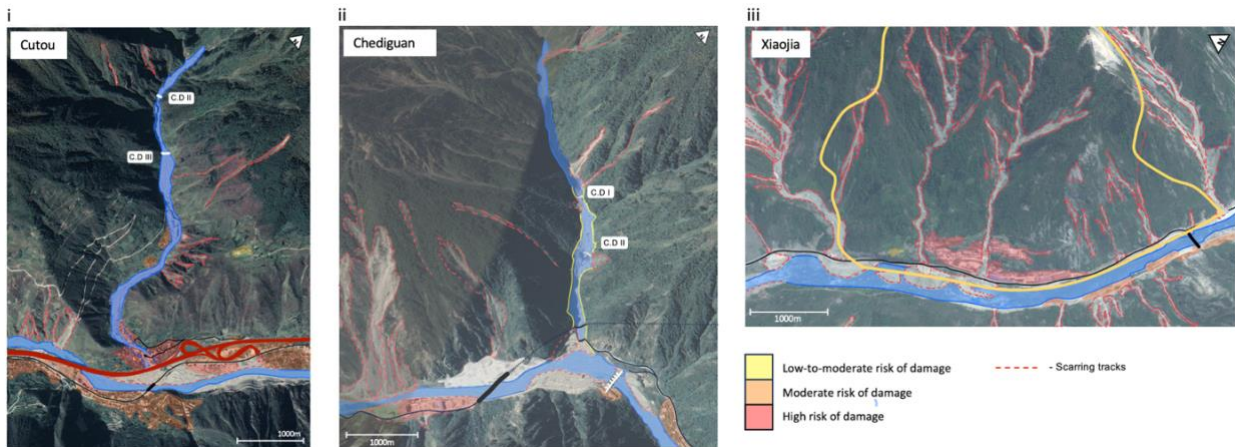
301
302
303
304
305
306
307
308
309

Analysis of satellite imagery from 2005 to 2019, and topographic profiles, reveals channel widening, deepening, aggradation, and deposition, likely attributed to the mobilisation of coseismic deposits and subsequent debris flow occurrences (Zhang et al., 2015; Wang et al., 2018) (Fig 3). These observations allowed us to determine the zones of erosion, transportation, and deposition for each gully and to track changes over time. Hydrological and geomorphological analysis examines landscape morphology to identify erosional and depositional features i.e., scarring, changes to river channel, sediment buildup (Fig 4). By integrating the above, we delineated erosion-prone areas, which permitted sediment transport routes to be approximated, and identify locations of sediment deposition along the hydrological profile.



310
311
312
313
314

Figure 3: Hydrological profiles for the 3 study sites. Dam locations approximated for Cutou (i) and Chediguan (ii) based on a combination satellite imagery. Streams and main tributaries are numbered to identify and reference key branches within each catchment. Catchment profiles have been segmented into 3 zones – ‘erosion’, ‘transportation’ and ‘deposition’ and key infrastructure annotated.



315 **Figure 4:** Satellite images of the 3 study locations highlighting areas of scarring from previous debris flow activity
 316 and areas of increased erosion (© Google Earth 2019). Dam locations have been approximated for Cutou (i) and
 317 Chediguan (ii). The built environment has been shaded based upon risk of damage based upon proximity to areas
 318 of high erosion. Critical infrastructure has been added where appropriate: black like represents the G4217 road
 319 with the thicker sections representing bridges and the dashed lines, tunnels. The red line in (i) is the G213
 320 Highway.
 321
 322

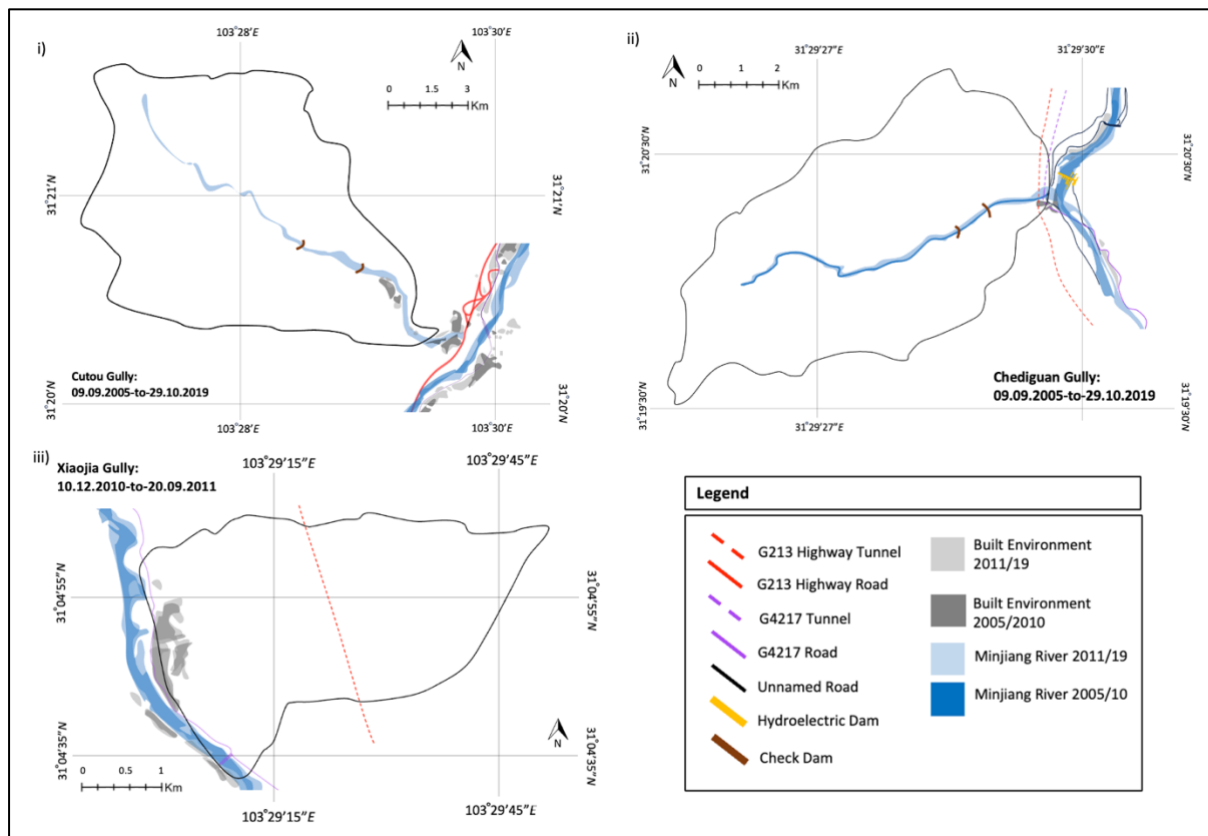
323 In Cutou and Chediguan, deposition patterns shifted post-earthquake, particularly following the construction of
 324 check dams. Increased deposition occurs behind check dams compared to meander bends and basal slopes of the
 325 debris fan, demonstrating the effective sediment trapping of the check dams (Wang et al., 2019). Regarding the
 326 erosion patterns in Xiaojia, we observed common patterns in the upper gully sections at higher elevations, with
 327 deposition occurring at the basal slopes. This is due to the absence of structural alterations to the channel,
 328 permitting sediment to be transported to the channel and subsequent river outlet directly. The deposition patterns
 329 in Cutou and Chediguan, are strongly controlled by the distribution of check dams, in the middle and downstream
 330 portions of the catchment (Wang et al., 2019). The complex interplay between natural and anthropogenic factors
 331 demonstrates the dynamic evolution of risk in post-earthquake catchments and highlights the role of check dams
 332 in both mitigating and potentially exacerbating risk.
 333

334 The landscape morphology prior to the 2008 earthquake was marked by extensive vegetation (over 70% of land
 335 cover) and minimal permanent engineered features. Cutou gully contained a widespread distribution of buildings
 336 along both the mid and lower slopes. Figure 5 shows the growth of the built environment between 2005 and 2019
 337 in Cutou and Chediguan and between 2010 to 2011 in Xiaojia. The built environment in Cutou is concentrated
 338 within the transportation and deposition zones on both sides on the stream. In Chediguan by comparison we
 339 observed fewer residential structures, mostly industry and some commercial structures. Additionally, buildings in
 340 the gully are more spread out than in Cutou highlighted by the isolated settlements to the south of the catchment
 341 and single industrial site situated in the basin. Post-2008, noticeable tracks of scarring from debris flows are
 342 concentrated downstream of dams 2 and 3 in Cutou (Fig 4(i)), and upstream of dams 1 and 2 in Chediguan (Fig
 343 4(ii)). Deposition patterns are evident downstream of all modifications, forming a depositional zone,
 344 encompassing approximately 15% and 20% of the built environment in 2019 within the transportation zone of
 345 Cutou and Chediguan, respectively.
 346

347 Xiaojia was chosen as the comparative catchment due to the absence of engineered mitigation such as check dams.
 348 This analysis of Xiaojia therefore enables comparisons on the effectiveness and limitations of engineering
 349 approaches applied to Cutou and Chediguan. In Xiaojia, the lack of engineered dam structures, results in different
 350 erosion and deposition patterns compared to the other two catchments. Distinct patterns of upstream erosion and
 351 downstream deposition are observed, contrasting with the more controlled environments in the modified gullies,
 352 where deposition occurs on the northern channel flank and pronounced erosion on the southern flank. The data
 353 availability for building types, quality and spatial distribution was limited to remote sensing images and few
 354 literature sources, which restricts our ability to thoroughly assess how specific building characteristics, such as
 355 materials, influence the exposure of the built environment to debris flow hazard. This is particularly evident in
 356 Xiaojia, where more specific input data would be beneficial for understanding the role of urbanisation and
 357 construction practices on risk levels.
 358

359 Our analysis of Xiaojia unveils no discernible relationship between building development and heightened
 360 exposure, particularly to residential and critical infrastructure. This lack of correlation is potentially linked to
 361 factors beyond simple urbanisation patterns, like construction quality, building regulations, presence of natural
 362 barriers, and effectiveness of mitigation measures. Natural terrain barriers observed in this gully including steep
 363 slopes and rocky outcrops, could limit the extent of debris flow impacts by reducing the mobility of debris and
 364 offering natural protection to certain areas. To fully understand this observation, further investigation into the
 365 above variables is warranted. The absence of significant urban expansion, particularly post-earthquake in Xiaojia
 366 may be a key factor in mitigating exposure. This area has experienced less intensive development compared to
 367 Cutou and Chediguan, where urban expansion following the implementation of check dams potentially increased
 368 exposure to debris flow hazards. Furthermore, the building quality and structural characteristics in Xiaojia may
 369 play a significant role in influencing its overall vulnerability and subsequent damage outcomes. Due to limited
 370 detailed building-specific data in terms of construction and materials, our assessment simplifies vulnerability to a
 371 binary classification based on observed damage and location. It is possible that buildings in Xiaojia may be of
 372 higher structural integrity or designed to withstand environmental stressors better than those in more developed
 373 catchments which would contribute to the observed exposure patterns.

374
 375 Additionally, detailed mapping of past debris flow events and their impacts on the built environment could provide
 376 insights into the specific mechanisms influencing vulnerability in Xiaojia. By conducting a more comprehensive
 377 analysis that considers these factors – especially in terms of land-use planning, construction standards and the role
 378 of natural terrain features at the local scale, we can gain a better understanding of the complex interactions between
 379 building development and exposure to natural hazards in Xiaojia. This, in turn, can inform more effective risk
 380 management and mitigation strategies tailored to the unique characteristics of the area. Development in Xiaojia
 381 primarily concentrates on the lower slopes (Fig 5(i) and (ii)) at the gully mouth, featuring the construction of
 382 major roads and highways (G213 and G2417), alongside the expansion of existing residential areas. Chediguan
 383 exhibits a less marked land cover transformation, owing to roads being directed through mountain tunnels. Xiaojia
 384 notably, development in Xiaojia mainly surges post-earthquake up to 2010, with only minor construction
 385 activities documented thereafter (Fig 5(iii); see also Supplementary Figures S3(i) and 3(ii))



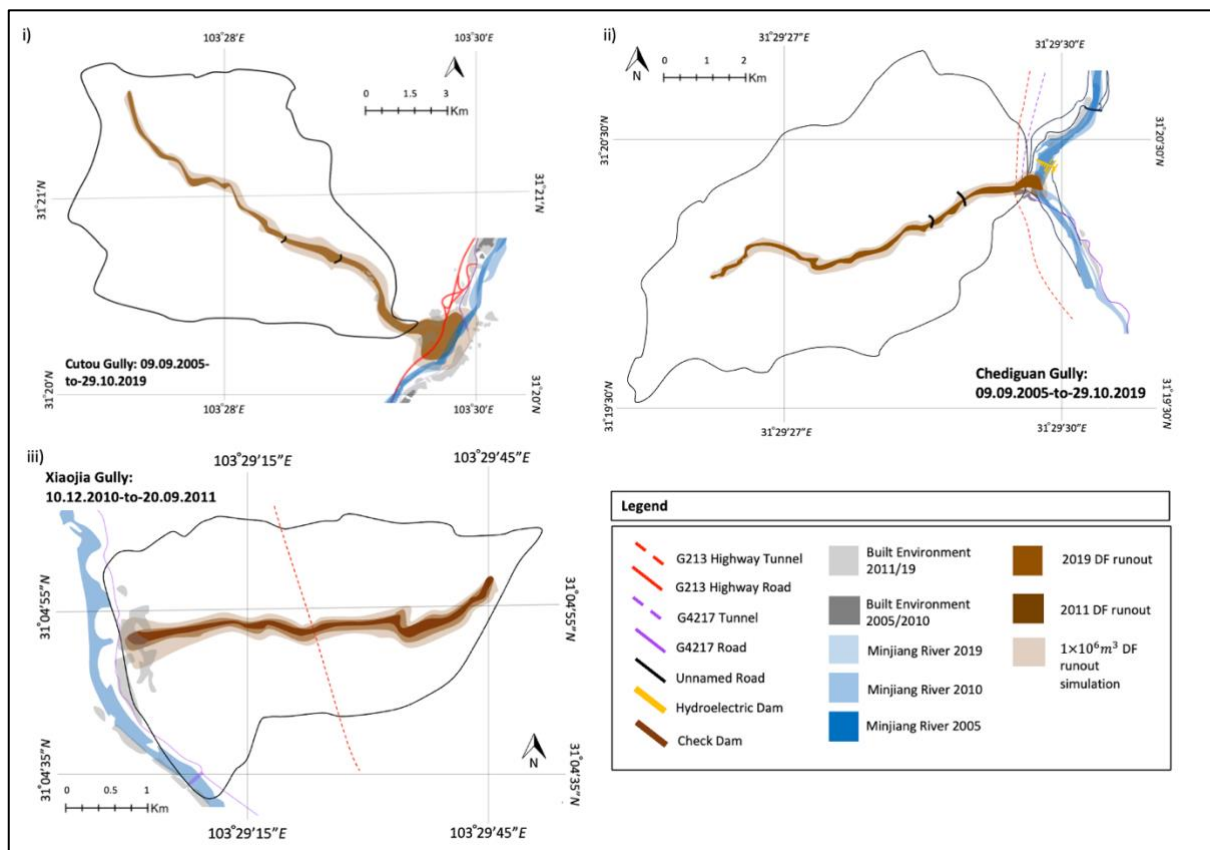
386 **Figure 5:** Evolution of the built environment and key infrastructure in (i) Cutou, (ii) Chediguan and (iii) Xiaojia
 387 post-earthquake between 2005 and 2019. Roads and tributary channels are annotated; all symbology is defined in
 388 the legend. In Cutou, pale blue shading indicates the mapped extent of a tributary channel post-2010 and does not
 389 imply absence in the earlier period. Several areas shown as built environment in 2005–2010 may have been
 390 damaged during debris flows, but limitations in imagery restrict differentiation between reconstruction and new

391 development in subsequent years. Scale bars have been corrected to reflect the true spatial extent of each
392 catchment.
393

394 We mapped the number of buildings impacted by debris flows that occurred within the Chediguan and Cutou
395 gullies. At 02:00 a large-scale debris flows hit Chediguan, impacting numerous structures, at around 05:00 a
396 similar debris flow hit Cutou with significant inundation noted. 79 of the 197 buildings (40%) in Cutou (Fig 5(i)
397 and Supplementary Figures S1(i) and (ii)) were impacted by the flow i.e., flooded, damaged, or destroyed.
398 Buildings in Chediguan were less impacted by that event with 7 out of the total 69 (10.1%) (see Supplementary
399 Figures S2(i) and (ii)). We combined the satellite imagery with the datasets produced by Wang (2022) which
400 supported our observations of check dam overtopping in both Cutou and Chediguan during the 2019 event. In
401 2011 a similar event in Xiaojia impacted approximately 5 of the 43 (11.6%) buildings in the gully (Fig 5(iii)).
402

403 4.3 Modelling exposure to post-earthquake debris flows

404 Our LAHARZ simulations demonstrate a clear correlation between exposure and debris flow runout, revealing a
405 notable increase in building damage as runout volumes escalate from low ($10,000\text{m}^3$) to high ($100,000\text{m}^3$) and
406 extreme ($1,000,000\text{m}^3$) scenarios across all catchments. Despite the presence of check dams, the 2019 debris flows
407 recorded runout volumes significantly larger than the maximum simulated volume, resulting in substantial
408 building and infrastructural loss in Cutou (Fig 6(i)) and Chediguan (Fig 6(ii)).
409
410
411



412 **Figure 6:** Debris flow runouts for 2019 in Cutou (i) and Chediguan(ii) and 2011 in Xiaojia (iii) underlain by the
413 extreme LAHARZ runout scenario. Low ($10,000\text{m}^3$) and high ($100,000\text{m}^3$) runouts are not displayed as they are
414 not easy to visualise at map scale.
415
416

417 While low ($10,000\text{m}^3$) and high ($100,000\text{m}^3$) volume runouts are not visually represented in figure 6 due to their
418 small spatial extent that do not clearly illustrate the influence of check dams – our analysis highlights their critical
419 role at the smaller scale. These smaller simulations demonstrate that check dams effectively reduce exposure
420 during low magnitude debris flow events, limiting damage to building and infrastructure in Cutou and Chediguan.
421 Thus, although not easily visualised at the map scale, the efficacy of check dams in mitigating small debris flow
422 events is not disputed by our results.

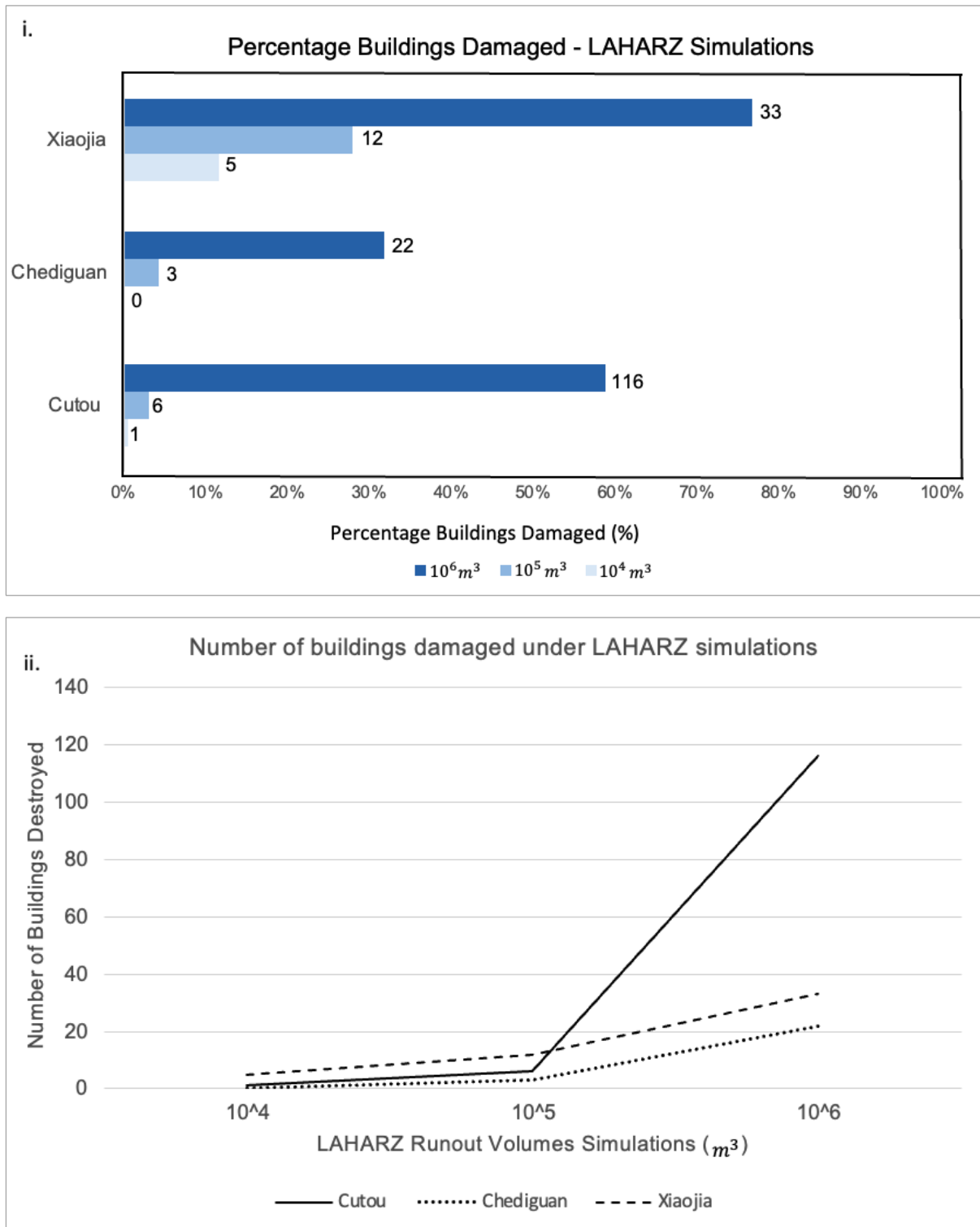
423 We examined the temporal dynamics of building changes within the three gullies in response to check dam
424 development, while also considering the implications of the levee effect (fig 6). Our simulations revealed the

425 effectiveness of engineered measures in mitigating exposure to debris flow events. In both Cutou and Chediguan,
426 the presence of check dams led to reduced exposure at low and high debris flow volumes (fig 7(i) and (ii)).
427 However, the mitigative structure provides no discernible protection against extreme debris flows. Notably, Cutou
428 consistently exhibited elevated exposure to debris flow runout compared to Chediguan. In contrast, the
429 unengineered Xiaojia (fig 6(iii)), shows a more consistent increase in exposure with debris flow volume,
430 illustrating the effectiveness of check dams at low and high debris flow volumes. This comparison underscores
431 how unmitigated gullies, like Xiaojia, experience greater susceptibility to debris flow damage compared to
432 engineered gullies like Cutou and Chediguan at the lower to moderate volume. It is important to clarify that Figure
433 6(iii) depicts the cumulative built environment up to 2019 in Xiaojia, including all infrastructure developed post-
434 2005. When we refer to “restrained expansion” in Xiaojia between 2011 and 2019, this relates specifically to the
435 comparatively limited rate and spatial extent of new built environment development during that period, as shown
436 in Figure 5. Xiaojia's post-2011 expansion appeared restrained, indicating a potential adaptive response following
437 debris flow events. In contrast, substantial expansion occurred in Cutou and Chediguan between 2011 and 2019,
438 despite experiencing a debris flow event in 2013, suggesting the impact of check dams implemented post-2013.
439

440 Furthermore, the incremental increase between high and extreme simulations in Xiaojia paralleled Chediguan's
441 gradual incline, diverging from Cutou's steep escalation. Xiaojia sustained a maximum building damage of 33%
442 under extreme scenarios, compared with 59% in Cutou and 22% in Chediguan. This discrepancy suggests that the
443 effectiveness of check dams may have limits under extreme debris flow events, highlighting that while check
444 dams may reduce damage at low to moderate volumes, they provide limited protection during extreme events.
445 Our observations underscore the nuanced variability in the effectiveness of check dams, influenced by contextual
446 factors and landscape characteristics.
447

448 However, it is important to note that our study only explores this hypothesis within a small sample, three
449 catchments, which contains the ability to generalise these findings. While the evidence points to a potential levee
450 effect associated with check dam construction and subsequent built environment expansion, further research across
451 a larger catchment sample is necessary. Expanding the scope of this analysis would help validate whether the
452 trends we have observed hold more broadly and improve understanding of socio-environmental feedback on risk
453 exposure and mitigation effectiveness.
454

455
456
457
458
459
460
461
462
463
464
465
466
467
468
469
470
471
472
473
474
475
476
477
478
479



481 **Figure 7:** Built environment impacts from three debris flow scenarios modelled using LAHARZ at Cutou,
 482 Chediguan and Xiaojia. (i). Percentage of buildings damaged as a proportion of total buildings (Cutou – 197,
 483 Chediguan – 69 and Xiaojia – 43) in each scenario. The numbers at the end of the bars are the number of buildings
 484 damaged buildings in that debris flow scenario. (ii) Total number of buildings damaged by each simulated debris
 485 flow.

486

487

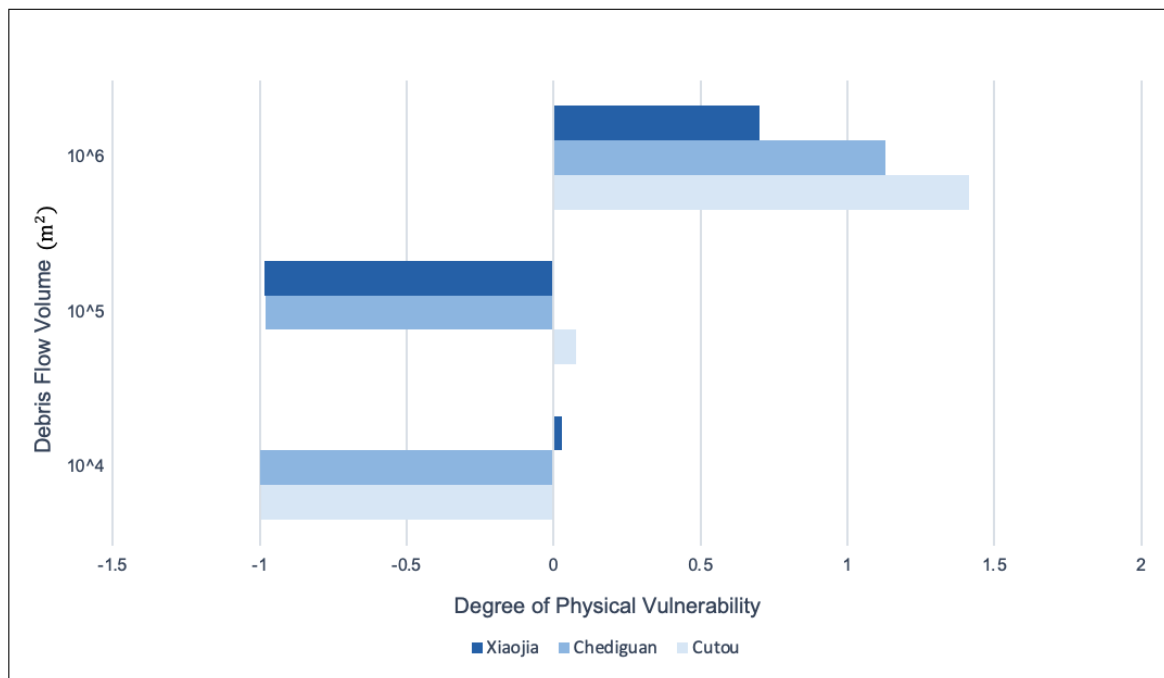
488 Figure 7 illustrates how a tenfold increase in runout volume corresponds to building damage, with a discernible
 489 rise in impacted building numbers noted between low and high scenarios, and a significant incline between high

490 and extreme scenarios across all catchments. The significant jump in destruction observed in Cutou between 10^5
 491 and 10^6 debris flow volume simulations is driven by the combined effect of the increased flow magnitude
 492 overwhelming the capacity of check dams and the spatial distribution of building within the flow path, leading to
 493 disproportionately higher damage. These simulations provide valuable insights into the efficacy of engineered
 494 mitigation structures. While check dams in Cutou and Chediguan effectively reduce exposure at low and high
 495 runoff volumes, concerns arise when surpassing the maximum capacity.
 496

497 We acknowledge the importance of decoupling debris flow inundation from building damage, as damage depends
 498 on various factors including but not limited to building materials and structural integrity, which are not controlled
 499 for in this analysis. Therefore, our assessment focuses primarily on exposure as a proxy for risk. Regarding the
 500 influence of check dams on sediment dynamics, these structures alter the distribution of erosion and deposition
 501 by trapping debris upstream (Figure 3), thereby reducing downstream sediment loads and runoff distances. This
 502 function contributes to reduced exposure in low to moderate debris flow scenarios but become less effective during
 503 extreme events when sediment volume exceeds retention capacity.
 504

505 Urbanisation emerges as a significant contributing factor impacting exposure and future risk, with the presence of
 506 check dams during the 2019 events significantly contributing to the built environment's exposure. However, due
 507 to the lack of available data on building materials in these three regions, we were unable to quantify their influence
 508 on structural vulnerability. To fully understand the effect of check dams and validate our statistical approach,
 509 comprehensive numerical analysis of multiple hazard events in each gully is necessary. This sub-section addresses
 510 the elements driving hazard-related risk scenarios, including the trigger event, return period, and level of damage,
 511 and underscores the importance of considering these factors when suggesting and implementing modifications.
 512

513 The exposure model is applied to historical events (2019 and 2011) and LAHARZ simulations, showcasing
 514 changes in the degree of exposure across the catchments with increasing debris flow runoff volumes (Fig 8).
 515 Consistent with earlier observations in exposure, Cutou exhibits a heightened vulnerability to debris flows at 64%
 516 after the 2019 event, followed by Chediguan at 52% and Xiaojia with 2% in 2011. A discernible change in building
 517 exposure is observed between the high and extreme scenarios across all catchments. The most influential factor
 518 in overall vulnerability remains the number of buildings, highlighting urbanization as a contributing factor
 519 impacting both exposure and physical vulnerability. Moreover, the presence of failed check dams in Cutou and
 520 Chediguan during the 2019 events significantly contributes to their physical vulnerability. These failures occurred
 521 primarily through overtopping of the dams, which exacerbated the impact of debris flows in these catchments.



522 **Figure 8:** Changes in the degree of exposure with increasing runoff volumes using the exposure model developed
 523 in equation 1. The 2011 and 2019 debris flows are also noted as a base marker from an observed hazard event.
 524
 525

526 **5. Discussion**

527 Post-earthquake structural interventions influence the volume and spatial distribution of sediment within the
528 catchment. Our observations show that check dams act as local depocentres within the catchment, often storing
529 large volumes of sediment upstream of the majority of building development. The choices made about post-
530 earthquake development of the built environment, particularly housing, and mitigative measures like check dams,
531 evolve rapidly without a clear approach to mitigating adverse long-term consequences of sediment retention
532 behind dams (McGuire et al., 2017). Additionally, the processes driving geological disasters in the complex
533 landscape of the Longmenshan occur at different timescales to the rapid socio-economic development in the region
534 (Chen et al., 2022).

535
536 Although our analysis focuses on smaller-scale communities, the implications drawn from our findings echo those
537 of broader studies. For instance, Arrogante-Funes et al. (2021)'s extensive investigation into hazard mitigation
538 strategies in larger geographical regions, drew parallels to the effectiveness and limitations of mitigation measures
539 to debris flows. Similarly, Chen et al. (2021) provided insights into the complexities of hazard mitigation,
540 emphasising the necessity of adaptive responses considering local contexts. This aligns with our analysis that each
541 gully must be assessed and mitigated individually rather than collectively to account for local geological and
542 hydrological influences on mitigation effectiveness. Moreover, Li et al. (2018) examined the long-term impact of
543 engineering interventions, noting the variability in check dams effectiveness over time. This supports our
544 conclusion that the diminishing effectiveness of check dams is likely the result of sediment accumulation and
545 structural degradation and highlights the necessity for their continued maintenance post-construction in addition
546 to adaptive mitigation strategies. Furthermore, Eidsvig et al. (2014) and Tang et al. (2011) explored the interplay
547 between socio-economic factors and hazard vulnerability, emphasising that community resilience is directly
548 linked to economic resource availability and social cohesion. This corroborates our understanding that debris flow
549 mitigation is a multifaceted issue, and socio-economic conditions are integral to their success. By situating our
550 findings within the broader context delineated by these studies, we accentuate the relevance and applicability of
551 our research beyond the confines of the specific communities under study.

552
553 Open check dams, similar to those established in Cutou and Chediguan, play a pivotal role in bed stabilization,
554 slope reduction, and the regulation of sediment transport (Bernard et al., 2019). However, inadequate
555 understanding of post-earthquake debris flow characteristics has led to the failure of many newly constructed
556 engineered structures to mitigate hazards effectively, amplifying damage instead (Chang et al., 2022). During the
557 August 2019 debris flow, Cutou experienced the highest inundation, with 40% of surveyed structures directly
558 affected, including critical infrastructure like the G4217 highway bridge. In Chediguan, despite a declined
559 industrial presence, compared to earlier periods i.e., during the construction of the hydroelectrical dam in the
560 Minjiang, debris flow impacts affected 7% of structures. The presence of check dams in both locations contributed
561 to raised exposure and hazard impacts during the 2019 event, with overtopping and damage to dam sections
562 recorded.

563
564 We conducted LAHARZ scenarios to predict potential exposure to debris flows with volumes that have been
565 observed within the catchments and the region. While it is intuitive that larger debris flows would affect a greater
566 areas, our results provide a quantified and site-specific correlation between exposure and debris flow runout,
567 showing notable increases in building damage as runout volumes escalated from low to extreme across all
568 catchments. This explicit demonstration is critical for understanding the scale of risk in these environments. We
569 observed two key elements to the role of check dams in affecting exposure to debris flows. When empty, check
570 dams are effective at mitigating the effects of small and medium volume debris flows. Yet, the check dams in
571 Cutou and Chediguan, are from our results, designed to mitigate small to medium debris flow volumes, which
572 limits their effectiveness against the extreme runout volumes denoted by our simulations. In other words, it is not
573 that check dams are inherently ineffective against large flows, but within the specific context of the mountainous
574 Sichuan landscape, they are insufficient to fully mitigate these extreme debris flow events. Additional simulations
575 without check dams at Cutou and Chediguan indicated that while check dams did reduce damage from smaller
576 events as shown in Figure 7, their failure during extreme events from overtopping or breaching can exacerbate
577 impacts releasing stored sediment, sometimes resulting in greater damage than scenarios without dams along
578 sections of the gully channel. Large runout volumes in the 2019 debris flows resulted in substantial building and
579 infrastructural loss in both Cutou and Chediguan, suggesting a negative contribution from damaged check dams.
580 Cutou was found to be highly exposed to extreme debris flow volumes, a result of its high degree of urban
581 development concentrated at the basal slopes.

582
583 The fact that Xiaojia was found to possess the least exposure to the most extreme debris flow volume suggests
584 that there may be an adaptive component to debris flow mitigation in catchments without significant check dam

585 development. These findings suggest that urban development and debris flow risk co-evolve based on the nature
586 of the structural interventions the studied areas.

587
588 Our analysis of erosion, transportation, and deposition zones for each gully revealed significant changes in
589 landscape morphology post-earthquake, likely attributed to mobilised coseismic deposits and subsequent debris
590 flow occurrences. The presence of check dams influenced deposition patterns, with mid-to-downstream trends
591 indicating effective sediment retention in Cutou and Chediguan, while Xiaojia exhibited typical erosion-
592 deposition behaviour. Our findings can be supported by a similar occurrence during the “8.13” debris flow event
593 in Wenjiagou. The damage and subsequent failure of mitigative check dams led to the inundation of 490 houses
594 or more recently, a debris flow in the Miansi and Weizhou townships on 27 June 2023 blocked the valley in the
595 first instance before breaching the dam and causing 7 fatalities (Petley., 2023). Further research is thus imperative
596 to devise appropriate mitigation approaches for post-seismic debris flows. Whilst existing literature has
597 underscored the physical effectiveness of check dams in reducing exposure to debris flow impacts within Alpine
598 terrains (Piton et al., 2016), it should be noted that their primary function extends beyond this to also provide
599 socio- economic and political reassurance (Wu et al., 2012; Chen et al., 2022)

600
601 The findings of our paper provide preliminary evidence supporting the theory of the levee effect by demonstrating
602 how the implementation of mitigative measures, such as check dams, can inadvertently increase exposure levels
603 and risk perception in hazard-prone areas. However, we acknowledge that our analysis is limited to three
604 catchments, and additional socio-economic and geographic factors may also encourage or discourage
605 development. Therefore, further research with a wider study sample is needed to fully substantiate. The interplay
606 between engineering solutions and the built environment as highlighted in our study through analysis of the 2011
607 and 2019 events as well as the LAHARZ simulations, illustrates the levee effect. Similar to previous studies on
608 flooding and the levee effect. Similar to previous studies on flooding, (e.g. Collenteur et al., 2015), our paper
609 suggests that the perceived reduction in hazard risk due to mitigative structures can lead to increased levels of
610 exposure due to raised development in debris flow-prone regions. This effect is particularly evident in the Cutou
611 catchment where urban expansion occurred post-dam construction, despite the repeated occurrence of high
612 magnitude debris flows. This suggests a distorted perception of hazard risk, which ultimately drives urbanisation
613 into vulnerable areas (Chen et al., 2015; Ao et al.,2020).

614
615 The levee effect can influence exposure to large-scale debris flow events by inadvertently increasing risk in areas
616 protected by engineered mitigation structures, such as check dams. This occurs because the perceived safety
617 provided by these structures can encourage development in vulnerable areas, which might otherwise remain
618 uninhabited due to their high-risk nature. This phenomenon is best evidenced in our paper by the Cutou catchment,
619 where the construction of check dams in 2013 coincided with widespread urban expansion, despite ongoing small-
620 scale debris flow activity in the area. It is also possible that the prioritisation of check dam construction was
621 influenced by pre-existing high levels of development, reflecting a reactive approach to hazard mitigation in
622 already urbanised zones. In our study, we have observed that the rate of urban expansion post-dam construction
623 increased. This raises an important question about the interplay between mitigation efforts and development
624 patterns, suggesting that structural interventions may both respond to and shape urban growth in hazard prone
625 areas. Subsequently, building exposure increased by 64% post-2008, underscoring the risk amplification
626 associated with structural mitigation. This observation highlights the necessity of coupling structural interventions
627 with strategies that address residual risks and foster community awareness of long-term hazard vulnerabilities.
628 The 2019 debris flow event exemplified the risks associated with this effect, as the flow overtopped the check
629 dams and used the stored material as a secondary fuel, significantly amplifying the impact. As a result, 40% of
630 surveyed buildings were inundated, demonstrating how the levee effect can potentially escalate exposure to large-
631 scale debris flow events.

632
633 Our LAHARZ simulations further reinforce the limitations of engineered structures as the sole mitigative measure
634 in alpine environments; urbanisation of mountainous terrains further complicates the balance between
635 technological advancements and geological hazards (Zhang, S et al., 2014; Zhang and Li., 2020; Luo et al., 2023).
636 Despite the presence of check dams, our extreme runout volume resulted in significant impacts on the built
637 environment in Cutou and Chediguan, including overtopping and dam failure. The use of these simulations
638 emphasises the challenges of reducing exposure to at-risk structures and highlights the unpredictable nature of
639 debris flow occurrences. Moreover, our findings relating to the altered patterns of erosion and deposition
640 emphasise the relationship between natural topography, engineered interventions, and risk perception in post-
641 seismic debris flows. Urbanisation exacerbates this complexity, influencing exposure and physical vulnerability
642 through deposit remobilisation. Our LAHARZ simulations serve as a practical demonstration of the levee effect,
643 illustrating how engineered structures may not provide adequate protection against runout volumes similar to the
644 extreme simulation, thereby reinforcing the importance of considering the levee effect in debris flow risk

645 management. The unpredictable nature of debris flow occurrences from pinpointing their location and timing to
646 ascertaining their volume and velocity ultimately means that the concept of the ‘levee effect’ remains core to the
647 issue of debris flows in post-seismic Sichuan (Cucchiaro et al., 2019a; Tang et al., 2022).

648
649 Whilst our findings are not able to definitively determine the prevalence of the levee effect with regards to
650 development in post-seismic environments like Sichuan, we hypothesise that the implementation of mitigative
651 structures like check dams may inadvertently increase exposure levels to large-scale debris flow events by creating
652 a false sense of safety. Although our investigation does not fully explore this phenomenon, our outcomes suggest
653 that the development of infrastructure in areas perceived to be safe due to the presence of engineered structures
654 may amplify hazard exposure. This highlights the limitations of solely relying on engineered interventions in
655 reducing exposure to at-risk structures under the extreme LAHARZ scenario. Furthermore, we highlighted the
656 complex interplay between engineering solutions and human behaviour, warranting further investigation
657 (Papathoma-Köhle et al., 2011; Gong et al., 2021). By emphasising the challenges and limitations of engineered
658 structures in mitigating debris flow impacts, we underscore the need for comprehensive risk management
659 strategies that consider the complexities of urbanization and flow-based hazards in mountainous terrains.

660
661 Despite the presence of these engineered interventions, our analysis demonstrates significant exposure levels and
662 infrastructure damage during extreme debris flow events. This discrepancy between perceived risk reduction and
663 actual hazard exposure underscores the need for a more comprehensive understanding of risk perception in the
664 context of hazard mitigation strategies. Moreover, our study highlights the importance of considering human
665 behaviour and decision-making processes in the design and implementation of risk management measures. Future
666 research should focus on elucidating the mechanisms driving risk perception in hazard-prone areas and developing
667 strategies to bridge the gap between perceived and actual risk to enhance the effectiveness of mitigation efforts.

668 669 670 **6. Conclusion**

671 Our study investigated the changing exposure to debris flows in Cutou Chediguan and Xiaojia since the 2008
672 Wenchuan earthquake. We used high resolution satellite imagery to build a time series of building inventories
673 between 2005 and 2019. Despite recurrent debris flow occurrences between 2010 to 2013, we observed increased
674 urban developments across all three gullies to varying extents until 2015.

675
676 We identified significant differences in the impacts of debris flow events in 2011 and 2019 respectively. In the
677 August 2019 debris flow, Cutou experienced the highest inundation, with 40% of surveyed structures directly
678 affected, including critical infrastructure such as the G4217 highway bridge. In contrast, the 2011 event in Xiaojia
679 impacted approximately 11.6% of buildings in the gully, indicating a lower level of damage compared to Cutou.
680 The presence of check dams in Cutou and Chediguan contributed to increased exposure and hazard impacts during
681 the 2019 event, with overtopping and damage to dam sections recorded at both locations. However, despite the
682 presence of these mitigative structures, the impact on the built environment was significant, suggesting limitations
683 in their effectiveness, particularly during extreme runout volumes. Our Laharz simulations demonstrated a clear
684 correlation between exposure and debris flow runout, revealing a notable increase in building damage as runout
685 volumes increased from low to high and finally extreme scenarios across all catchments. Despite the presence of
686 check dams, the simulations indicated that these structures were unable to reduce the impacts on the built
687 environment, especially during extreme events. Furthermore, our analysis highlighted a heightened level of built
688 environment exposure in Cutou compared to Chediguan and Xiaojia driven by urbanisation, the presence of
689 critical infrastructure, and the effectiveness of mitigative measures.

690
691 Our findings suggest that the presence and location of check dam in gully channels likely increased building
692 exposure by fostering a perception of reduced hazard risk, thereby contributing to a levee effect. This raises
693 concerns about the long-term implications, including structural integrity, maintenance and clearing. LAHARZ
694 modelling provides comprehension of check dam efficacy, raising concerns for Cutou and Chediguan in high-to-
695 extreme runout events. Further, the combined use of the LAHARZ GIS toolkit and exposure analysis contributes
696 to a holistic understanding of the risk landscape, informing strategies for enhanced disaster resilience and
697 sustainable development in vulnerable areas.

698
699 The assumptions and subsequent considerations highlighted throughout our study underscore the complexities of
700 how check dams, as a mitigative structure, influences land-use planning and development in hazard-prone areas.
701 These factors ensure that the data outputs are comprehensive but also reflective of the inherent complexities of
702 the study area and limitations in available data sources and analytical tools. We have highlighted a relationship
703 between the presence of engineered measures like check dams alongside the built environment, showing how this
704 relationship has contributed to increased debris flow impacts post-2008 earthquake in Sichuan, particularly

705 provinces along the Minjiang. Our results emphasise the need for a multi-faceted approach to risk management,
706 integrating socio-economic development and addresses the paradoxical role of mitigative structures in shaping
707 public perception to hazard exposure and vulnerability. Understanding these complexities is vital for informed
708 decision-making and effective debris flow risk management.

709
710 Overall, our findings have indicated that the 2019 debris flow events caused more significant damage and higher
711 exposure levels compared to the 2011 flow, emphasising the need for comprehensive risk management strategies
712 in debris flow-prone areas.

713 714 **Acknowledgements**

715 EH is supported by the BGS-NERC National Capability grant ‘Geosciences to tackle Global Environmental
716 Challenges’ (NERC reference NE/X006255/1) and publishes with permission from the Executive Director of the
717 British Geological Survey.

718 719 **References**

720 Ao, Y., Huang, K., Wang, Y., Wang, Q. and Martek, I. 2020. Influence of built environment and risk
721 perception on seismic evacuation behavior: Evidence from rural areas affected by Wenchuan
722 earthquake. *International journal of disaster risk reduction: IJDRR* 46(101504), p. 101504. Available at:
723 <https://www.sciencedirect.com/science/article/pii/S2212420919313500>.

724
725 Arrogante-Funes, P., Bruzón, A.G., Arrogante-Funes, F., Ramos-Bernal, R.N. and Vázquez-Jiménez, R.
726 2021. Integration of vulnerability and hazard factors for landslide risk assessment. *International journal of*
727 *environmental research and public health* 18(22), p. 11987. Available at:
728 <http://dx.doi.org/10.3390/ijerph182211987>.

729
730 Bernard, M., Boreggio, M., Degetto, M. and Gregoretti, C. 2019. Model-based approach for design and
731 performance evaluation of works controlling stony debris flows with an application to a case study at Rovina di
732 Cancia (Venetian Dolomites, Northeast Italy). *The Science of the total environment* 688, pp. 1373–1388.
733 Available at: <https://www.sciencedirect.com/science/article/pii/S0048969719325288>.

734
735 Brown, C. F. *et al.* Dynamic world, near real-time global 10 m land use land cover mapping. *Scientific Data* 9,
736 251 (2022)

737
738 Chang, M., Luo, C., Wu, B. and Xiang, L. 2022. Catastrophe process of outburst debris flow triggered by the
739 landslide dam failure. *Journal of hydrology* 609(127729), p. 127729. Available at:
740 <https://www.sciencedirect.com/science/article/pii/S0022169422003043>.

741
742 Chen, N.-S., Hu, G.-S., Deng, M.-F., Zhou, W., Yang, C.-L., Han, D. and Deng, J.-H. 2011. Impact of
743 earthquake on debris flows — a case study on the Wenchuan earthquake. *Journal of earthquake and*
744 *tsunami* 05(05), pp. 493–508. Available at: <http://dx.doi.org/10.1142/s1793431111001212>.

745
746 Chen, X., Cui, P., You, Y., Chen, J. and Li, D. 2015. Engineering measures for debris flow hazard mitigation
747 in the Wenchuan earthquake area. *Engineering geology* 194, pp. 73–85. Available at:
748 <https://www.sciencedirect.com/science/article/pii/S0013795214002579>.

749
750 Chen, M. *et al.* 2021. Quantitative assessment of physical fragility of buildings to the debris flow on 20 August
751 2019 in the Cutou gully, Wenchuan, southwestern China. *Engineering geology* 293(106319), p. 106319.
752 Available at: <https://www.sciencedirect.com/science/article/pii/S0013795221003306>

753
754 Chen, Y., Song, J., Zhong, S., Liu, Z. and Gao, W. 2022. Effect of destructive earthquake on the population-
755 economy-space urbanization at county level—a case study on Dujiangyan county, China. *Sustainable cities and*
756 *society* 76(103345), p. 103345. Available at: <http://dx.doi.org/10.1016/j.scs.2021.103345>.

757
758 Collenteur, R. A., de Moel, H., Jongman, B., & Di Baldassarre, G. 2015. The failed-levee effect: Do societies
759 learn from flood disasters? *Natural Hazards (Dordrecht, Netherlands)*, 76(1), 373–388.
760 <https://doi.org/10.1007/s11069-014-1496-6>

761
762 Costa, J.E. 1984. Physical geomorphology of debris flows. In: *Developments and Applications of*
763 *Geomorphology*. Berlin, Heidelberg: Springer Berlin Heidelberg, pp. 268–269. Available at:
764 http://dx.doi.org/10.1007/978-3-642-69759-3_9.

765
766 Couvert, B., Lefebvre, B., Lefort, P., & Morin, E. 1991. Etude générale sur les seuils de correction torrentielle
767 et les plages de dépôts. *Houille Blanche*, 77(6), 449–456. <https://doi.org/10.1051/lhb/1991043>
768
769 Cruden, D.M. and Varnes, D.J. 1996. Landslides: Investigation and Mitigation. Chapter 3—Landslide Types
770 and Processes. Transportation research board special report, 247. In: Transportation research board special
771 report (247).
772
773 Cucchiaro, S. et al. 2019a. Geomorphic effectiveness of check dams in a debris-flow catchment using multi-
774 temporal topographic surveys. *Catena* 174, pp. 73–83. Available at:
775 <https://www.sciencedirect.com/science/article/pii/S0341816218304910>.
776
777 Cucchiaro, S., Cazorzi, F., Marchi, L., Crema, S., Beinat, A. and Cavalli, M. 2019b. Multi-temporal analysis of
778 the role of check dams in a debris-flow channel: Linking structural and functional
779 connectivity. *Geomorphology (Amsterdam, Netherlands)* 345(106844), p. 106844. Available at:
780 <https://www.sciencedirect.com/science/article/pii/S0169555X1930323X>.
781
782 Cui, P., Wei, F. Q., He, S. M., You, Y., Chen, X. Q., Li, Z. L., et al. 2008. Mountain Disasters Induced by the
783 Earthquake of May 12 in Wenchuan and the Disasters Mitigation. *J. Mountain Sci.* 26 (3), 280–282.
784 doi:10.35123/geo-expo_2017_4
785
786 Dai, Z., Huang, Y., Cheng, H. and Xu, Q. 2017. SPH model for fluid–structure interaction and its application to
787 debris flow impact estimation. *Landslides* 14(3), pp. 917–928. Available at: [http://dx.doi.org/10.1007/s10346-](http://dx.doi.org/10.1007/s10346-016-0777-4)
788 [016-0777-4](http://dx.doi.org/10.1007/s10346-016-0777-4).
789
790 Eidsvig, U.M.K., Papathoma-Köhle, M., Du, J., Glade, T. and Vangelsten, B.V. 2014. Quantification of model
791 uncertainty in debris flow vulnerability assessment. *Engineering geology* 181, pp. 15–26. Available at:
792 <https://www.sciencedirect.com/science/article/pii/S0013795214002051>.
793
794 Fan, X. et al. 2018. What we have learned from the 2008 Wenchuan Earthquake and its aftermath. A decade of
795 research and challenges. *Engineering geology* 241, pp. 25–32. Available at:
796 <https://www.sciencedirect.com/science/article/pii/S0013795218307233>.
797
798 Fan, X., Scaringi, G., Domènech, G., Yang, F., Guo, X., Dai, L., He, C., Xu, Q., and Huang, R. 2019a. Two
799 multi-temporal datasets that track the enhanced landsliding after the 2008 Wenchuan earthquake, *Earth Syst.*
800 *Sci. Data*, 11, 35–55, <https://doi.org/10.5194/essd-11-35-2019>
801
802 Fan, X., Scaringi, G., Korup, O., West, A. J., van Westen, C. J., Tanyas, H., Niels Hovius, Tristram C. Hales,
803 Randall W. Jibson, Kate E. Allstadt, Limin Zhang, Stephen G. Evans, Chong Xu, Gen Li, Xiangjun Pei,
804 Qiang Xu, and Runqiu Huang. 2019b. Earthquake-induced chains of geologic hazards: Patterns, mechanisms,
805 and impacts. *Reviews of Geophysics*, 57, 421–503. <https://doi.org/10.1029/2018RG000626>
806
807 Farr, T. G., et al. 2007. The Shuttle Radar Topography Mission, *Rev. Geophys.*, 45, RG2004,
808 doi:10.1029/2005RG000183.
809
810 Fell, R., Corominas, J., Bonnard, C., Cascini, L., Leroi, E., & Savage, W. Z. 2008. Guidelines for landslide
811 susceptibility, hazard, and risk zoning for land use planning. *Engineering Geology*, 102(3–4), 85–98.
812 <https://doi.org/10.1016/j.enggeo.2008.03.022>
813
814 Francis, O. Fan, X., Hales, T., Hobbey, D., Xu, Q., Huang, R. 2022. ‘The fate of sediment after a large
earthquake’, *Journal of Geophysical Research: Earth Surface*, 127(3). doi:10.1029/2021jf006352
815
816 Gong, X.-L., Chen, X.-Q., Chen, K.-T., Zhao, W.-Y. and Chen, J.-G. 2021. Engineering planning method and
817 control modes for debris flow disasters in scenic areas. *Frontiers in earth science* 9. Available at:
<http://dx.doi.org/10.3389/feart.2021.712403>
818
819 Google Earth Pro. Version 9.189.0.0 “Location of Cutou gully, Chediguan Gully and Xiaojia Gully,
Sichuan, China”. Image taken 2020. Accessed June 2, 2023.

- 820 Guo, X., Cui, P., Li, Y., Ma, L., Ge, Y., and Mahoney, W.B. 2016. Intensity–duration threshold of rainfall-
821 triggered debris flows in the Wenchuan Earthquake affected area, China. *Geomorphology* (Amsterdam,
822 Netherlands) 253, pp. 208–216. Available at: <http://dx.doi.org/10.1016/j.geomorph.2015.10.009>.
- 823 Guzzetti, F. et al. 2008. The rainfall intensity-duration control of shallow landslides and debris flows: An
824 update. *Landslides* 5(1), pp. 3–17. [Doi: 10.1007/s10346-007-0112-1](https://doi.org/10.1007/s10346-007-0112-1).
- 825 Hao, P. Hooimeijer, P. Sliuzas, R and Geertma, S. 2013. ‘What drives the spatial development of urban villages
826 in China?’, *Urban Studies*, 50(16), pp. 3394–3411. doi:10.1177/0042098013484534
- 827 Hao, P. 2012. *Spatial evolution of urban villages in Shenzhen*. dissertation. University of Utrecht. Available at:
828 https://webapps.itc.utwente.nl/librarywww/papers_2012/phd/puhao.pdf
- 829 He, N., Fu, Q., Zhong, W., Yang, Z., Cai, X. and Xu, L. 2022. Analysis of the formation mechanism of debris
830 flows after earthquakes – A case study of the Legugou debris flow. *Frontiers in ecology and evolution* 10.
831 Available at: <http://dx.doi.org/10.3389/fevo.2022.1053687>
- 832 Horton, A.J. et al. 2019. ‘Identifying post-earthquake debris flow hazard using Massflowx’, *Engineering*
833 *Geology*, 258, p. 105134. doi:10.1016/j.enggeo.2019.05.011
- 834 Hu, K.H., Cui, P., and Zhang, J.Q. 2012. Characteristics of damage to buildings by debris flows on 7 August
835 2010 in Zhouqu, Western China. *Natural hazards and earth system sciences* 12(7), pp. 2209–2217. Available
836 at: <https://nhess.copernicus.org/articles/12/2209/2012/nhess-12-2209-2012.pdf>.
- 837
838 Huang, R. Q., & Li, W. L. 2009. Analysis of the geo-hazards triggered by the 12 May 2008 Wenchuan
839 Earthquake, China. *Bulletin of Engineering Geology and the Environment*, 68(3), 363–371.
840 <https://doi.org/10.1007/s10064-009-0207-0>
- 841
842 Huang, R., Pei, X., Fan, X., Zhang, W., Li, S. and Li, B. 2012. The characteristics and failure mechanism of
843 the largest landslide triggered by the Wenchuan earthquake, May 12, 2008, China. *Landslides* 9(1), pp. 131–
844 142. Available at: <http://dx.doi.org/10.1007/s10346-011-0276-6>.
- 845
846 Huang, R. and Li, W. 2014. Post-earthquake landsliding and long-term impacts in the Wenchuan earthquake
847 area, China. *Engineering geology* 182, pp. 111–120. Available at:
848 <http://dx.doi.org/10.1016/j.enggeo.2014.07.008>.
- 849
850 Hübl, J. and Fiebiger, G. 2005. Chap. 18 - Debris-flow mitigation measures. In: *Debris-flow Hazards and*
851 *Related Phenomena*. Berlin, Heidelberg: Springer Berlin Heidelberg, pp. 445–487. Available at:
852 https://link.springer.com/content/pdf/10.1007/3-540-27129-5_18.pdf
- 853
854 Ivanov, P., Geological Institute, Bulgarian Academy of Sciences, Acad. Georgi Bonchev Str., Bl. 24, 1113
855 Sofia, Bulgaria, Dobrev, N., Berov, B., Frantzova, A., Krastanov, M., Nankin, R., Geological Institute,
856 Bulgarian Academy of Sciences, Acad. Georgi Bonchev Str., Bl. 24, 1113 Sofia, Bulgaria, & Geological
857 Institute, Bulgarian Academy of Sciences, Acad. Georgi Bonchev Str., Bl. 24, 1113 Sofia, Bulgaria. (2022).
858 Landslide risk for the territory of Bulgaria by administrative districts. *Geologica Balkanica*, 51(3), 21–28.
859 <https://doi.org/10.52321/geolbalc.51.3.21>
- 860
861 Iverson, R.M., Schilling, S.R., and Vallance, J.W., 1998, Objective delineation of areas at risk from inundation
862 by lahars: *Geological Society of America Bulletin*, V 110, no.8, p. 972-984.
- 863
864 Jiang, W., Deng, Y., Tang, Z., Cao, R., Chen, Z. and Jia, K. 2016. Adaptive capacity of mountainous rural
865 communities under restructuring to geological disasters: The case of Yunnan Province. *Journal of rural*
studies 47, pp. 622–629. Available at: <http://dx.doi.org/10.1016/j.jrurstud.2016.05.002>.
- 866
867 Kean, J.W. et al. 2019. Inundation, flow dynamics, and damage in the 9 January 2018 Montecito debris-flow
868 event, California, USA: Opportunities and challenges for post-wildfire risk assessment. *Geosphere* 15(4), pp.
1140–1163. Available at: <http://dx.doi.org/10.1130/ges02048.1>.

- 869 Li, C., Wang, M. and Liu, K. 2018. A decadal evolution of landslides and debris flows after the Wenchuan
870 earthquake. *Geomorphology* (Amsterdam, Netherlands) 323, pp. 1–12. Available at:
871 <http://dx.doi.org/10.1016/j.geomorph.2018.09.010>.
- 872 Li, N., Tang, C., Zhang, X., Chang, M., Shu, Z. and Bu, X. 2021b. Characteristics of the disastrous debris flow
873 of Chediguan gully in Yinxing town, Sichuan Province, on August 20, 2019. *Scientific reports* 11(1). Available
874 at: <https://www.nature.com/articles/s41598-021-03125-x>
- 875 Liu, J., You, Y., Chen, X., Liu, J. and Chen, X. 2014. Characteristics and hazard prediction of large-scale
876 debris flow of Xiaojia Gully in Yingxiu Town, Sichuan Province, China. *Engineering geology* 180, pp. 55–67.
877 Available at: <https://www.sciencedirect.com/science/article/pii/S0013795214000702>
- 878 Liu, J., You, Y., Chen, X. and Chen, X. 2016. Mitigation planning based on the prediction of river blocking by
879 a typical large-scale debris flow in the Wenchuan earthquake area. *Landslides* 13(5), pp. 1231–1242. Available
880 at: <http://dx.doi.org/10.1007/s10346-015-0615-0>
- 881 Liu, J., Mason, P.J. and Bryant, E.C. 2018. Regional assessment of geohazard recovery eight years after the
882 Mw7.9 Wenchuan earthquake: a remote-sensing investigation of the Beichuan region. *International journal of*
883 *remote sensing* 39(6), pp. 1671–1695. Available at: <http://dx.doi.org/10.1080/01431161.2017.1410299>.
- 884 Luo, H.Y., Fan, R.L., Wang, H.J., and Zhang, L.M. 2020. Physics of building vulnerability to debris flows,
885 floods, and earth flows. *Engineering geology* 271(105611), p. 105611. Available at:
886 <https://www.sciencedirect.com/science/article/pii/S0013795219322227>.
- 887 Luo, H.Y., Zhang, L.M., Zhang, L.L., He, J., and Yin, K.S. 2023. Vulnerability of buildings to landslides: The
888 state of the art and future needs. *Earth-science reviews* 238(104329), p. 104329. Available at:
889 <https://www.sciencedirect.com/science/article/pii/S0012825223000181>.
- 890 Mattia Marconcini, Annetkatrin Metz-Marconcini, Thomas Esch and Noel Gorelick. Understanding Current
891 Trends in Global Urbanisation - The World Settlement Footprint Suite. *GI_Forum* 2021, Issue 1, 33-38 .2021.
892 Available at: <https://austriaca.at/0xc1aa5576%200x003c9b4c.pdf>
- 893 McGuire, L.A., Rengers, F.K., Kean, J.W. and Staley, D.M. 2017. Debris flow initiation by runoff in a recently
894 burned basin: Is grain-by-grain sediment bulking or en masse failure to blame?: DEBRIS FLOW
895 INITIATION. *Geophysical research letters* 44(14), pp. 7310–7319. Available at:
896 <http://dx.doi.org/10.1002/2017gl074243>.
- 897 OpenStreetMap contributors. OpenStreetMap database [PostgreSQL via API]. OpenStreetMap Foundation:
898 Cambridge, UK. 2024 [cited 20 Jul 2023]. © OpenStreetMap contributors. Available under the Open Database
899 Licence from: [openstreetmap.org](https://www.openstreetmap.org). Data mining by Overpass turbo. Available at <https://www.openstreetmap.org>
- 900 Papathoma-Köhle, M., Kappes, M., Keiler, M. and Glade, T. 2011. Physical vulnerability assessment for alpine
901 hazards: state of the art and future needs. *Natural hazards* (Dordrecht, Netherlands) 58(2), pp. 645–680.
902 Available at: <http://dx.doi.org/10.1007/s11069-010-9632-4>.
- 903 Peng, M., Zhang, L.M., Chang, D.S. and Shi, Z.M. 2014. Engineering risk mitigation measures for the landslide
904 dams induced by the 2008 Wenchuan earthquake. *Engineering geology* 180, pp. 68–84. Available at:
905 <https://www.sciencedirect.com/science/article/pii/S0013795214000696>.
- 906
907 Petley, D. 2023. *The 27 June 2023 landslide at Miansi, Sichuan Province, China*. Available at:
908 <https://blogs.agu.org/landslideblog/2023/06/29/miansi-landslide-1/>
- 909
910 Shen, P., Zhang, L. M., Chen, H. X., & Gao, L. 2017. Role of vegetation restoration in mitigating hillslope
911 erosion and debris flows. *Engineering Geology*, 216, 122–133. <https://doi.org/10.1016/j.enggeo.2016.11.019>
- 912 Shu, B., Chen, Y., Amani-Beni, M. and Zhang, R. 2022. Spatial distribution and influencing factors of
913 mountainous geological disasters in southwest China: A fine-scale multi-type assessment. *Frontiers in*
914 *environmental science* 10. Available at: <http://dx.doi.org/10.3389/fenvs.2022.1049333>.

- 915 Tang, C., Rengers, N., van Asch, T.W.J., Yang, Y.H. and Wang, G.F. 2011. Triggering conditions and
 916 depositional characteristics of a disastrous debris flow event in Zhouqu city, Gansu Province, northwestern
 917 China. *Natural hazards and earth system sciences* 11(11), pp. 2903–2912. Available at:
 918 <https://nhess.copernicus.org/articles/11/2903/2011/nhess-11-2903-2011.pdf>.
 919
- 920 Tang, C., Van Westen, C.J., Tanyas, H. and Jetten, V.G. 2016. Analysing post-earthquake landslide activity
 921 using multi-temporal landslide inventories near the epicentral area of the 2008 Wenchuan earthquake. *Natural*
 922 *hazards and earth system sciences* 16(12), pp. 2641–2655. Available at: [http://dx.doi.org/10.5194/nhess-16-](http://dx.doi.org/10.5194/nhess-16-2641-2016)
 923 [2641-2016](http://dx.doi.org/10.5194/nhess-16-2641-2016).
 924
- 925 Tang, Y. et al. 2022. Assessing debris flow risk at a catchment scale for an economic decision based on the
 926 LiDAR DEM and numerical simulation. *Frontiers in earth science* 10. Available at:
 927 <http://dx.doi.org/10.3389/feart.2022.821735>
 928
- 929 Thouret, J.-C., Antoine, S., Magill, C. and Ollier, C. 2020. Lahars and debris flows: Characteristics and
 930 impacts. *Earth-science reviews* 201(103003), p. 103003. Available at:
 931 <http://dx.doi.org/10.1016/j.earscirev.2019.103003>.
 932
- 933 Wang, C., Li, S. and Esaki, T. 2008. GIS-based two-dimensional numerical simulation of rainfall-induced
 934 debris flow. Available at: <https://nhess.copernicus.org/articles/8/47/2008/nhess-8-47-2008.pdf>
- 935 Wei, L., Hu, K. and Liu, J. 2022. Automatic identification of buildings vulnerable to debris flows in Sichuan
 936 Province, China, by GIS analysis and Deep Encoding Network methods. *Journal of flood risk*
 937 *management* 15(4). Available at: <http://dx.doi.org/10.1111/jfr3.12830>
- 938 Wei, L., Hu, K. and Liu, J. 2021. ‘Quantitative analysis of the debris flow societal risk to people inside
 939 buildings at different times: A case study of Luomo Village, Sichuan, Southwest China’, *Frontiers in Earth*
 940 *Science*, 8. doi:10.3389/feart.2020.627070.
- 941 Wei, L., Hu, K.-H. and Hu, X.-D. 2018. Rainfall occurrence and its relation to flood damage in China from
 942 2000 to 2015. *Journal of mountain science* 15(11), pp. 2492–2504. Available at:
 943 <http://dx.doi.org/10.1007/s11629-018-4931-4>
- 944 World Settlement Footprint Evolution data (1985-2015) ©DLR [cited Jul 2023]. 2019 All rights
 945 reserved. <https://geoservice.dlr.de/web/maps/eoc:wsfevolution>
 946
- 947 Yan, Y., Ge, Y.G., Zhang, J.Q. and Zeng, C. 2014. Research on the debris flow hazards in Cutou Gully,
 948 Wenchuan County on July 10, 2013. *Journal of Catastrophology*, 29(3), pp.229-234.
- 949 Zeng, Q.L., Yue, Z.Q., Yang, Z.F. and Zhang, X.J. 2009. A case study of long-term field performance of
 950 check-dams in mitigation of soil erosion in Jiangjia stream, China. *Environmental geology* 58(4), pp. 897–911.
 951 Available at: <http://dx.doi.org/10.1007/s00254-008-1570-z>.
- 952 Zeng, C., Cui, P., Su, Z., Lei, Y. and Chen, R. 2015. Failure modes of reinforced concrete columns of buildings
 953 under debris flow impact. *Landslides* 12(3), pp. 561–571. Available at: [http://dx.doi.org/10.1007/s10346-014-](http://dx.doi.org/10.1007/s10346-014-0490-0)
 954 [0490-0](http://dx.doi.org/10.1007/s10346-014-0490-0)
- 955 Zhang, S. 2014. Assessment of human risks posed by cascading landslides in the Wenchuan earthquake area.
 956 (Hong Kong): Hong Kong University of Science and Technology.
- 957 Zhang, Z. and Li, Y. 2020. Coupling coordination and spatiotemporal dynamic evolution between urbanization
 958 and geological hazards—A case study from China. *The Science of the total environment* 728(138825), p.
 959 138825. Available at: <http://dx.doi.org/10.1016/j.scitotenv.2020.138825>.
- 960 Zhu, Cheng, Bao, Chen, and Huang. 2022. Shaking table tests on the seismic response of slopes to near-fault
 961 ground motion. *Geomechanics and engineering* 29(2), pp. 133–143. Available at:
 962 <http://dx.doi.org/10.12989/gae.2022.29.2.133>.

963 Zou, Q., Cui, P., He, J., Lei, Y. and Li, S. 2019. Regional risk assessment of debris flows in China—An HRU-
964 based approach. *Geomorphology* (Amsterdam, Netherlands) 340, pp. 84–102. Available at:
965 <https://www.sciencedirect.com/science/article/pii/S0169555X19301849>
966
967

968 **Statements & Declarations**

969 **Conflict of Interest**

970 The authors disclose no financial or non-financial interests of competing interest during the preparation of this
971 manuscript.
972

973 **Author Contribution**

974 All authors contributed to the study conception and design. Material preparation, data collection and analysis were
975 performed by Isabelle Utley, Tristram Hales and Ekbal Hussain. The first draft of the manuscript was written by
976 Isabelle Utley and all authors commented on previous versions of the manuscript. All authors read and approved
977 the final manuscript
978
979